Subwavelength metrology of Al wire grating employing finite difference time domain method and Mueller matrix polarimeter

Adhikari, Achyut; Dev, Kapil; Asundi, Anand

2016

Adhikari, A., Dev, K., & Asundi, A. (2016). Subwavelength metrology of Al wire grating employing finite difference time domain method and Mueller matrix polarimeter. Interferometry XVIII, 9960, 99600F-. doi:10.1117/12.2240639

https://hdl.handle.net/10356/90175

https://doi.org/10.1117/12.2240639

Subwavelength metrology of Al wire grating employing finite difference time domain method and Mueller matrix polarimeter

Achyut Adhikari[a], Kapil Dev[a], Anand Asundi[a],
[a]*Centre for Optical and Laser Engineering, School of Mechanical and Aerospace Engineering, Nanyang Technological University, 50 Nanyang Avenue, Singapore 639798*

e-mail:adhi0005@e.ntu.edu.sg
Fax/Phone: 6790 5564

Abstract

Wire grid polarizers (WGP), are sub-wavelength gratings with applications in display projection system due to their compact size, wide field of view and long-term stability. Measurement and testing of these structures are important to optimize their use. This is done by first measuring the Mueller Matrix of the WGP using a Mueller Matrix Polarimeter. Next the Finite Difference Time Domain (FDTD) method is used to simulate a similar Mueller matrix thus providing the period and step height of the WGP. This approach may lead to more generic determination of sub-wavelength structures including diffractive optical structures.

1. Introduction

The miniaturization and advancement in technology poses a challenge in optical metrology and imaging systems to measure subwavelength structures with high dynamic speed and robustness. Most metrological equipment in semiconductor rely on electrical measurement, optical microscopy, scanning electron microscopy (SEM) and other probe microscopy techniques for such measurement. Several microscopic techniques with significant purpose measures in sub-micron scale on the virtue of versatility, simplicity and speed. Normal microscope is inefficient on resolution and precision for structures at or below 0.5 μm due to Rayleigh diffraction limit. Scanning tunneling microscopy is convenient for high resolution in three dimension but limited to conductive samples and slow measurement speed. SEM is best suited to measure semiconductors with high resolution but needs a vacuum environment which makes it complex and ultra-expensive [1]. Currently, various indirect methods are being explored for such as scatterometry and ellipsometry for rapid, full-field non-destructive testing[2, 3]. Polarization based methods are also being explored as it is well-known that sub-wavelength structures affect the State of Polarization[4, 5]. Changes in polarization can be quantified by the Mueller matrix which can measure parameters such as depolarization, retardance and diattenuation for complex anisotropic samples. The Mueller matrix can deal with any state of polarization (partially polarized, completely polarized or depolarized) compared to Jones matrix which works only with completely polarized light [6, 7]. Transmitted light through wire grid polarizer is analyzed by polarization state analyzer (PSA)

Interferometry XVIII, edited by Katherine Creath, Jan Burke, Armando Albertazzi Gonçalves Jr., Proc. of SPIE Vol. 9960, 99600F · © 2016 SPIE · CCC code: 0277-786X/16/$18 · doi: 10.1117/12.2240639

comprising a quarter wave plate and analyzer. MMP approach is only limited to the samples having periodic nano-structure. The 16 Mueller matrix obtained through MMP for WGP experimentally is compared to the computationally obtained finite difference time domain (FDTD) method.

2. Wire grid polarizer characterization

Normal dichroic polarizers employed in LCD absorb approximately 60% of the light produced at the bottom resulting in poor brightness. WGPs reflect unwanted light whereas traditional dichroic polarizers absorb it. WGPs consist of a periodic array of parallel metallic wires in a plane perpendicular to incident beam on the transparent substrate with a period or pitch of around 150nm, which is approximately three times smaller than the wavelength of light (400-800) nm. The pitch of the grating in WGP is less than the wavelength of light overcoming the Rayleigh diffraction limit by exhibiting no diffraction [8]. This periodic subwavelength structure in the WGP induces form birefringence. When unpolarized light is incident on the sample, the electric field component parallel to wire induces electron movement along the wire cumulatively reflected as a thin metal sheet parallel to grid wires. Whereas, the electric field component perpendicular to WGP passes through because of air gap thickness between the metallic grid wires. The Mueller Matrix Polarimeter (MMP) is used to measure the surface profile of WGP at 550 nm wavelength. The WGP has a size 25×25 *mm* and is sandwiched between glass substrates making it difficult to measure using an optical microscope (Rayleigh Diffraction Limit) and probe based microscope (wire grids covered by protective glass substrate) methods. Measurement of WGP using the MMP involves two significant steps. First, the 16 Mueller matrix elements are measured by varying the azimuthal angle of incident polarized light. The resulting Mueller matrix elements are compared with numerically simulated grating with different linewidths and periods of wire grids using Finite Difference Time Domain (FDTD).

3. Mueller matrix polarimeter

The Mueller matrix for an ideal polarizer in terms of the azimuthal angle (θ) is given by equation (1) where last row and column vector has null value [11]. These will be used as basis for comparison of the Mueller matrix for the Wire Grid Polarizer (WGP)

$$M_{Polarizer} = \begin{bmatrix} 1 & \cos 2\theta & \sin 2\theta & 0 \\ \cos 2\theta & \cos^2 2\theta & \sin 2\theta \cos 2\theta & 0 \\ \sin 2\theta & \sin 2\theta \cos 2\theta & \sin^2 2\theta & 0 \\ 0 & 0 & 0 & 0 \end{bmatrix} \quad (1)$$

To determine the 16 elements of a Mueller Matrix a Mueller Matrix Polarimeter (MMP) was used as shown in Fig. 1. Different states of polarization are generated by the Polarization State Generator (PSG) comprising of a polarizer and quarter wave plate. This polarization state is altered by the sample and analyzed by the Polarization State Analyzer (PSA)[9].

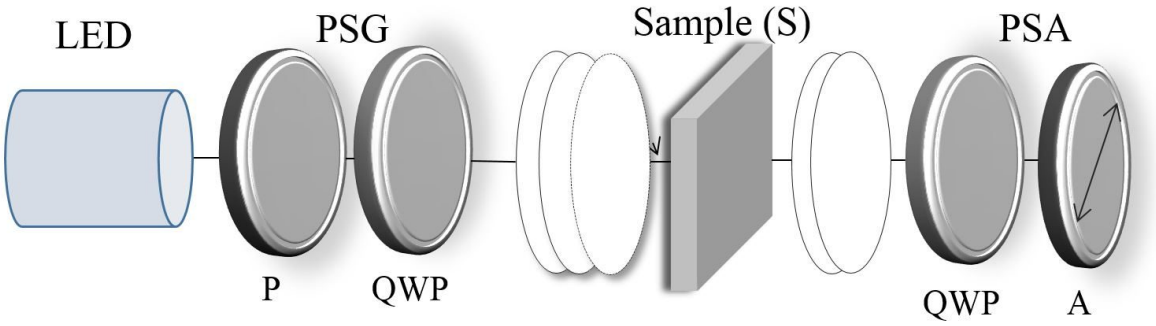

Figure 1: Mueller matrix polarimeter (MMP) with Sample (S) sandwiched between tunable PSG and PSA elements. (P- Polarizer, QWP – Quarter Wave Plate and A – Analyzer)

The incident light from a 550 nm LED is transmitted through PSG, then altered by the sample and finally analyzed by PSA. The Mueller Matrix [10] can be determined by recording 36 images with various state of polarization (SOPs) generated by PSG and analyzed by the PSA as in equation (2)

$$M = \begin{bmatrix} HH+HV+VH+VV & HH+HV-VH-VV & PH+PV-MH-MV & RH+RV-LH-LV \\ HH-HV+VH-VV & HH-HV-VH+VV & PH-PV-MH+MV & RH-RV-LH+LV \\ HP-HM+VP-VM & HP-HM-VP+VM & PP-PM-MP+MM & RP-RM-LP+LM \\ HR-HL+VR-VL & HR-HL-VR+VL & PR-PL-MR+ML & LL-RL-LR+RR \end{bmatrix} \quad (2)$$

Where H, V, P, M, R, L indicate Horizontal, Vertical, +45^o, -45^o, Right Circular and Left Circular Polarization. The first character is the input SOP generated by the PSG and second is the PSA SOP Hence HH would thus correspond to both input and output having the same horizontal polarization state. Initially, the Mueller matrix of air as shown in equation (3) is determined to calibrate system and quantify errors.

$$M_{Air} = \begin{bmatrix} 1.0000 & 0.0232 & 0.0014 & -0.0024 \\ 0.0232 & 0.9827 & 0.0582 & -0.0012 \\ -0.0043 & -0.0512 & 0.9942 & -0.0283 \\ -0.0119 & 0.0978 & -0.0118 & 0.9249 \end{bmatrix} \quad (3)$$

Next the WGP was used as a sample and placed on rotation stage between the PSG and PSA. The WGP was rotated at 10 degree interval recording 36 intensity images at every orientation till 180 degrees. The Mueller matrix values obtained by equation (2) for various azimuthal angles for ideal polarizer show good correlation to the experimentally obtained values from the Wire Grid Polarizer (WGP) as shown in Fig. 2. This suggests that the WGP behaves as expected like a polarizer. However, to characterize the structure of the WGP from this data requires solution of an inverse problem. To achieve this which an alternate approach is adopted. The Mueller matrix for different line widths and pitch of the subwavelength structure are simulated using Finite Difference Time Domain (FDTD). These are then compared with the experimentally obtained values to obtain the best match.

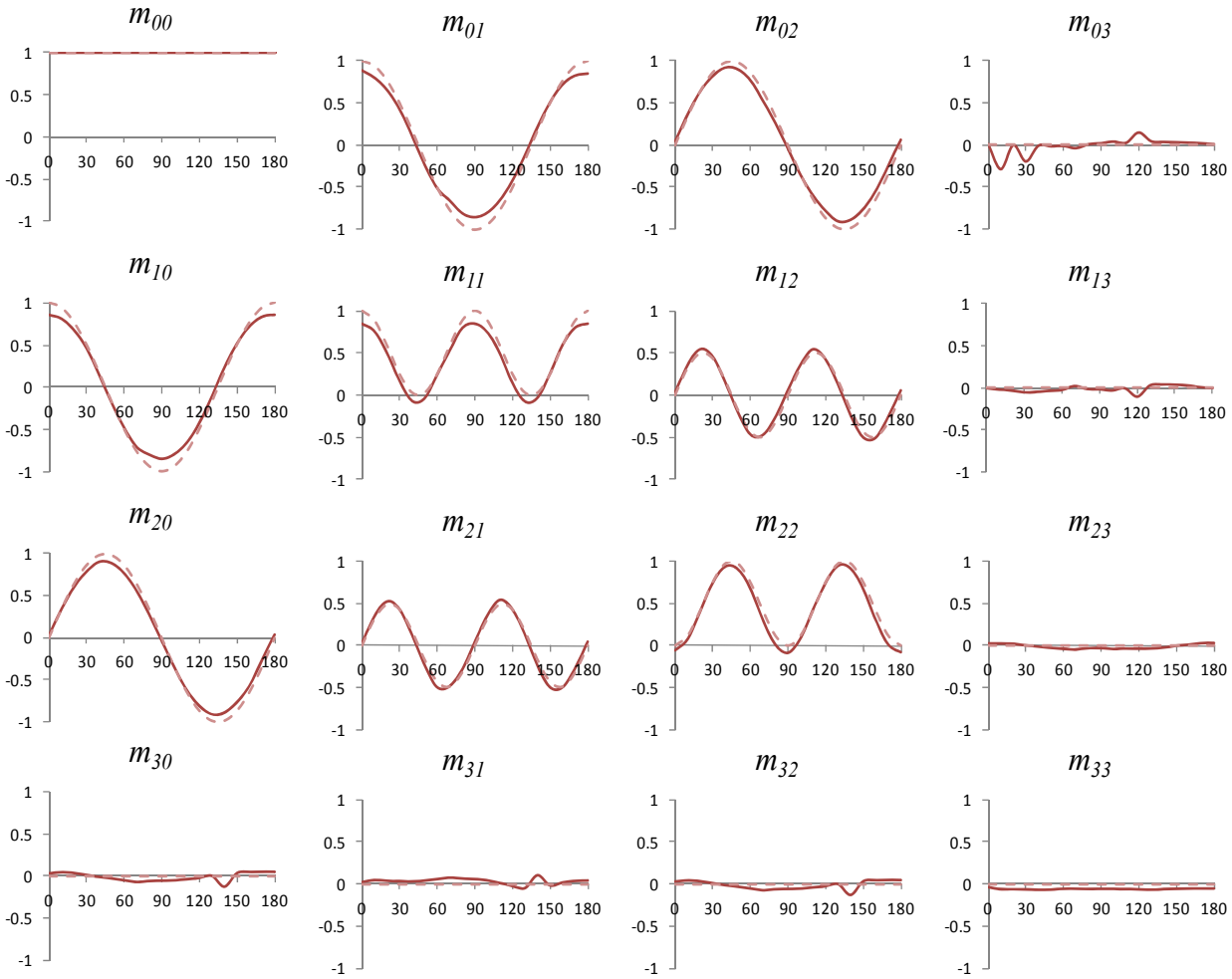

Figure 2: Mueller matrix elements variation at various azimuthal angle for WGP using MMP (Dashed line shows matrix element variation for an ideal polarizer)

4. Lumerical FDTD simulation analysis

This method involves the design of mechanical nanostructure and implementing Maxwell equation with constraints to predict its optical properties. There are two well-known computational electrodynamics modeling methods, viz. finite difference time domain (FDTD) and rigorous coupled wave analysis (RCWA) [12] based on time domain and frequency domain method respectively. Finite difference time domain (FDTD) method has become the state of the art for computing Maxwell's equations in complex geometries. This method is discrete in both space, time and vectorial approach for obtaining time and frequency domain information useful for problems and applications in electromagnetics and photonics. Optical properties, such as PER (Polarization Extinction Ratio) and transmission are varied by tuning the grating pitch, duty cycle and height of grating[14]. PER is the ratio

of maximum transmission for p-polarization to the minimum transmission of s-polarization and the duty cycle is percentage ratio of linewidth and pitch of the grating (eqn (4)).

$$\text{PER} = \frac{\textbf{Intensity at p state polarization } (I_p)}{\textbf{Intensity at s state polarization } (I_s)}, \qquad \text{Duty cycle} = \frac{\textbf{Linewidth of grating}}{\textbf{Pitch of grating}} \times \mathbf{100}\% \qquad (4)$$

The schematic of the simulated Al grating on glass substrate of refractive index 1.44 identifying the linewidth, height and pitch, is shown in Figure (3). The linewidth and pitch of Al grating are crucial parameters for various polarization states as stated in equation (4). The linewidth of grating should be less than 150 nm for polarizer to operate in the visible range. Simulation for a WGP with a duty cycle of 50% gives a transmission of 85% with PER approaching 4×10^6. The duty cycle is thus maintained at 50% throughout with a grating height of 200 nm.

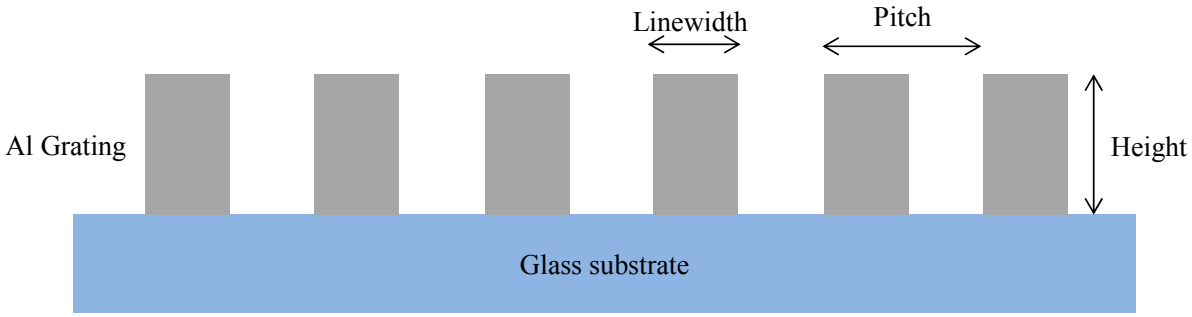

Figure 3: Schematic diagram of various important parameters in simulation setup

The linewidth is varied from 20 nm to 120 nm in the steps of 10 nm and changes in Mueller matrix element values are recorded. Various polarization states are generated by combining two orthogonal polarized plane wave sources with different relative amplitude and phase. Different SOPs generated on the Lumerical FDTD simulation setup with various amplitude and phase constructed are shown in Table 1.

Symbol	Polarization	Source 1 amplitude	Source 2 amplitude	Relative phase
⟹	Horizontal (H)	1	0	0
⇑	Vertical (V)	0	1	0
⇗	$+45^0$ (P)	1	1	0

	Right circularly polarized (R)	1	1	90^0

Table 1: Various SOPs generated by two orthogonal polarized plane waves

One of the limitations of the Lumerical FDTD is that circularly polarized light cannot be defined in terms of mueller matrix, hence it is given in terms of the incident stokes vector. Stokes vector for incident horizontal polarization, vertical polarization, 45^0 polarization and right circularly polarized can be given by $\boldsymbol{S_H}$ = {**1**; **1**; 0; 0}, $\boldsymbol{S_V}$ = {**1**; **-1**; 0; 0}, $\boldsymbol{S_P}$ = {**1**; 0; **1**; 0}, and $\boldsymbol{S_R}$ = {**1**; 0; 0; **1**} respectively. The Mueller matrix of WGP changes incident SOP, thus exiting SOPs can be given by Equation (6). Later, the obtained resultant stokes vector (S') is manipulated to achieve Mueller matrix characteristics of simulated WGP as in equation 10.

$$M = [M_0 \quad M_1 \quad M_2 \quad M_3] \tag{5},$$

$$M = \begin{pmatrix} m_{00} & m_{01} & m_{02} & m_{03} \\ m_{10} & m_{11} & m_{12} & m_{13} \\ m_{20} & m_{21} & m_{22} & m_{23} \\ m_{30} & m_{31} & m_{32} & m_{33} \end{pmatrix} \quad S = \begin{pmatrix} S_H \\ S_V \\ S_P \\ S_R \end{pmatrix}$$

$$\text{S'=MS} = \begin{pmatrix} m_{00} & m_{01} & m_{02} & m_{03} \\ m_{10} & m_{11} & m_{12} & m_{13} \\ m_{20} & m_{21} & m_{22} & m_{23} \\ m_{30} & m_{31} & m_{32} & m_{33} \end{pmatrix} \cdot \begin{pmatrix} S_H \\ S_V \\ S_P \\ S_R \end{pmatrix} = \begin{pmatrix} S'_H \\ S'_V \\ S'_P \\ S'_R \end{pmatrix} \tag{6}$$

The Mueller matrix elements $M_0 = [m_{00};\ m_{10};\ m_{20};\ m_{30}]$, $M_1 = [m_{01};\ m_{11};\ m_{21};\ m_{31}]$, $M_2 = [m_{02};\ m_{12};\ m_{22};\ m_{32}]$ and $M_3 = [m_{03};\ m_{13};\ m_{23};\ m_{33}]$ represents four column Mueller matrix elements. Thus, exiting Stokes vector on implementing equations (5) and (6) for the corresponding incident SOP are,

$$\boldsymbol{S'_H} = M_0 + M_1 \tag{7}$$

$$\boldsymbol{S'_V} = M_0 - M_1 \tag{8}$$

$$\boldsymbol{S'_P} = M_0 + M_2 \tag{9}$$

$$\boldsymbol{S'_R} = M_0 + M_3 \tag{10}$$

From the above four equation, equation (5) can be rewritten as,

$$M = \frac{1}{2}[(S'_H + S'_V) \quad (S'_H - S'_V) \quad 2S'_P - (S'_H + S'_V) \quad 2S'_R - (S'_H + S'_V)] \tag{11}$$

Mueller matrix for WGP calculated from exiting stokes vector is well formulated in Equation (11) implemented in simulation setup. Periodic boundary condition in *x* and *y*-direction are used in this simulation as well as perfectly matched layers (PML) in the z direction. PML fully absorb the electromagnetic field to avoid back reflection. The conformal minimum mesh size of 0.25 nm is implemented, although smaller size would have provided better results at the expense of computational time.

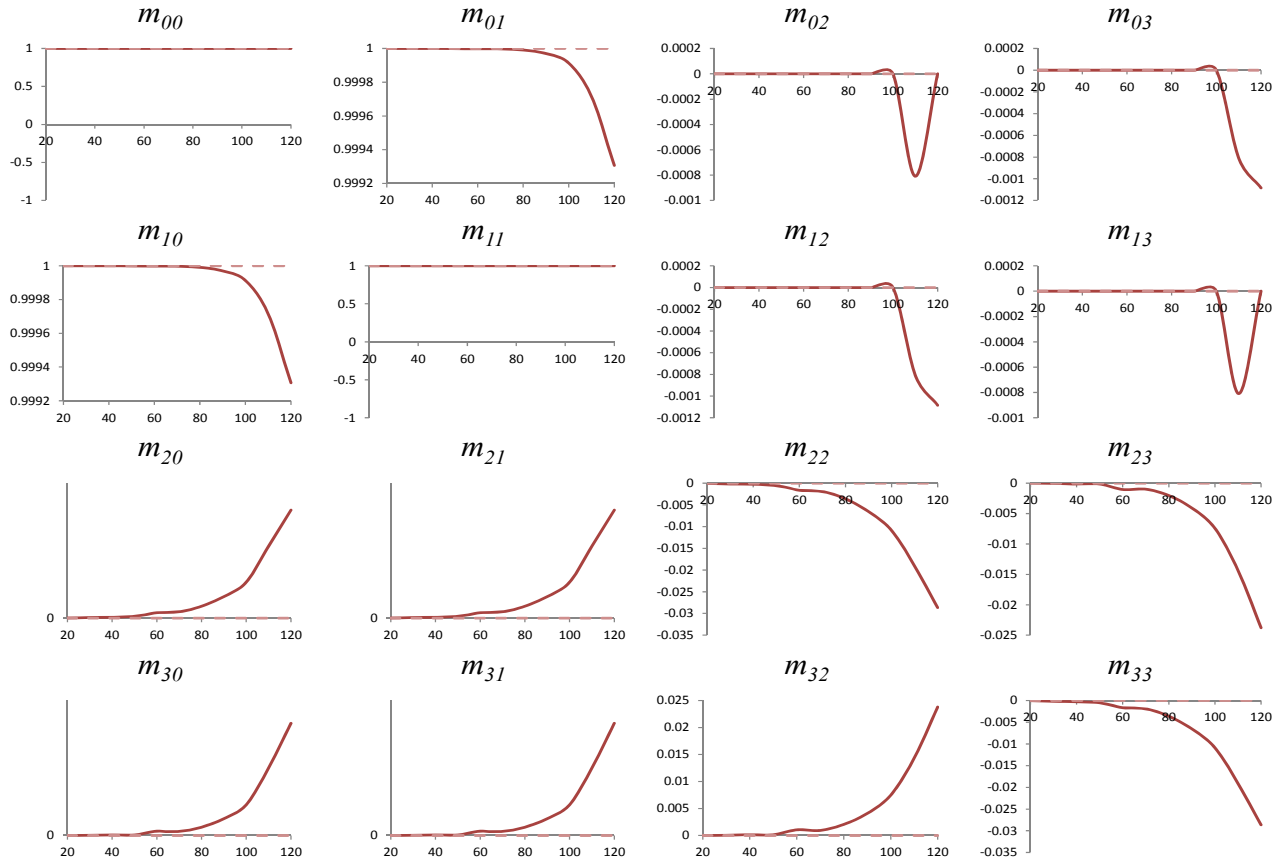

Figure 4: Mueller matrix elements variation for varying Al wire linewidth. (Dashed line shows matrix element variation for an ideal polarizer)

Figure 4 shows the Mueller Matrix elements for varying linewidth. From this figure, Mueller matrix elements deviate from their ideal values after linewidth exceeds 70 nm. Figure 5 shows the Mueller Matrix elements variation at different azimuth angles for three different linewidths (30nm, 40nm, 50 nm) were simulated. Two orthogonal plane polarized wave sources are fixed while the grating rotated from 0 to 180 degrees in steps of 10 degrees. The mesh settings, boundary conditions and duty cycle of 50% is kept as in the previous

simulation. Comparing the simulated values with the experimental data in Fig. 2, shows that the 40 nm linewidth provides the best fit as shown in Fig. 6. While this data compared just three different linewidths, it narrows down the search which can be further improved with linewidth variations around this value. However, this is at the expense of computational effort and convergence. The main advantage of using MMP is it provides more variables for a better fit and convergence. Thus, from various aspects it help to investigate overlay defects, characterizing line edge roughness, optical properties of anisotropic materials [15-17].

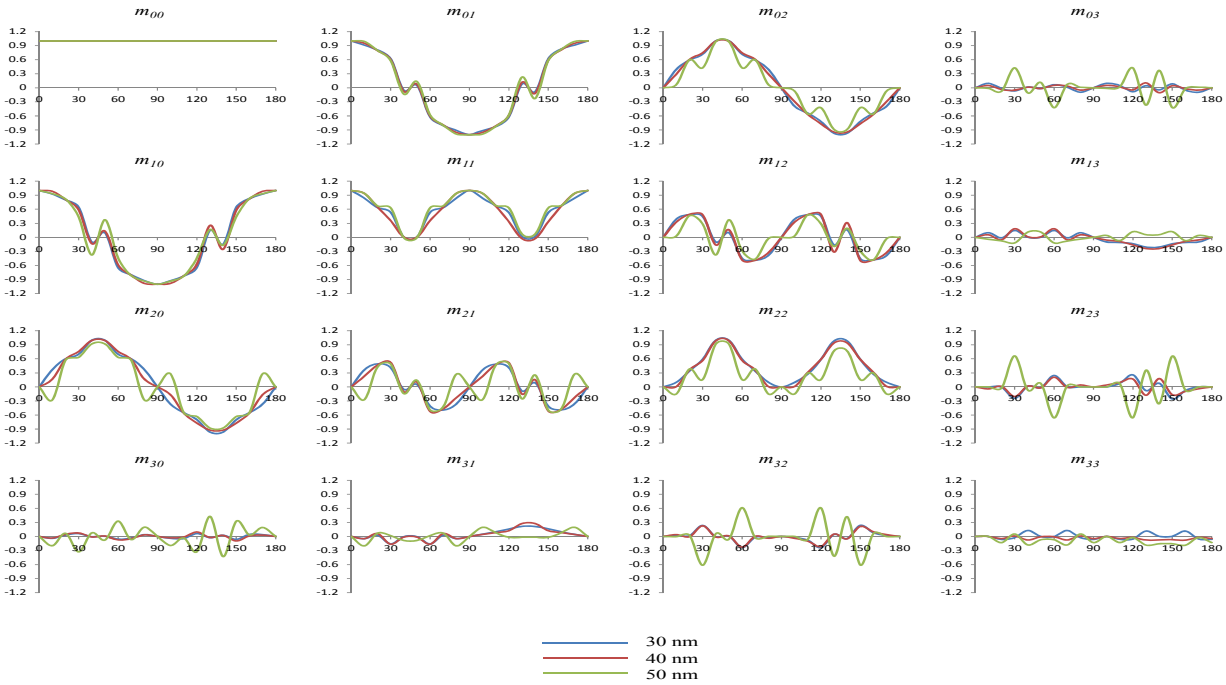

Figure 5: Mueller matrix elements variation in azimuthal rotation angle for different linewidths

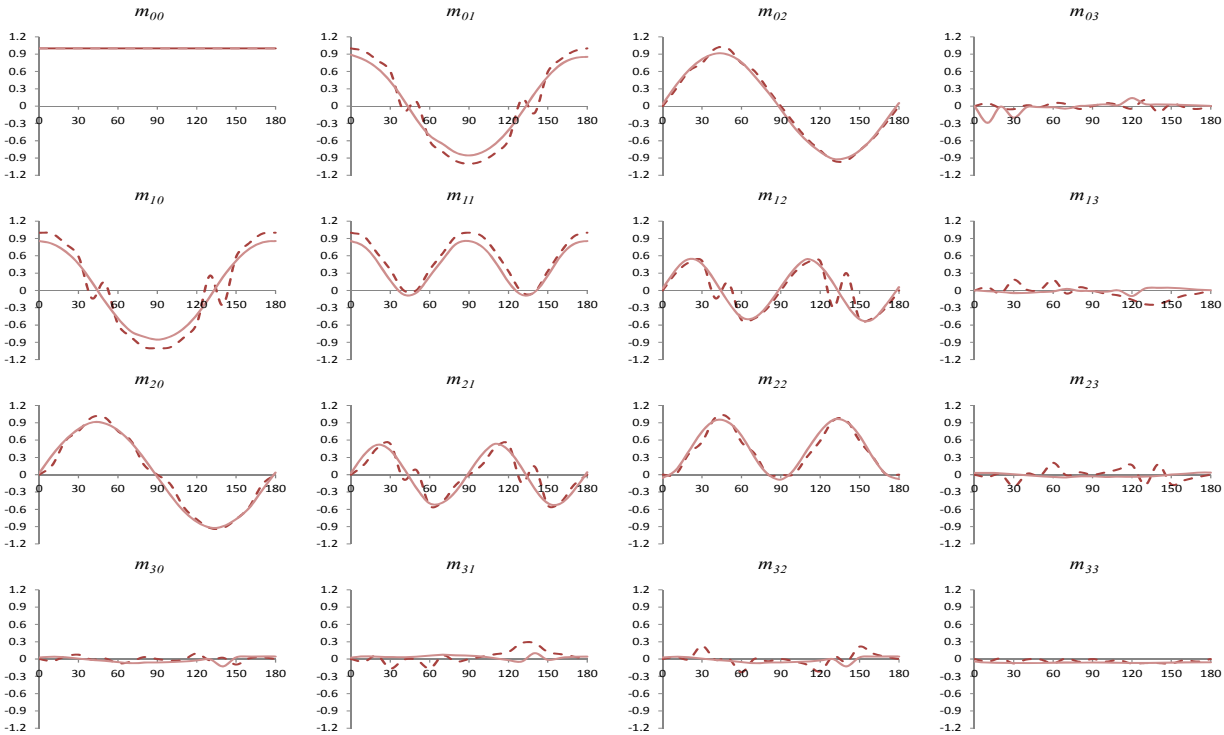

Figure 6: Comparison of Mueller matrix elements variation calculated experimentally using MMP and simulated FDTD (Dashed line represents simulated matrix element variation).

5. Conclusion

In this article, characterization of sub-wavelength structures using MMP and FDTD approach is proposed. The signature (Mueller matrix) of the sub-wavelength sample is first experimentally calculated using a Mueller matrix polarimeter. FDTD is then used to simulate the Mueller Matrix of different structures to find a best match. In the present case, the line width for a commercial WGP are determined using this approach and found to be around 40 nm with a 50% duty cycle and 200 nm height.

References

1. Raymond, C.J., et al., *Metrology of subwavelength photoresist gratings using optical scatterometry.* Journal of Vacuum Science & Technology B, 1995. **13**(4): p. 1484-1495.

2. Raymond, C.J., et al., *Multiparameter grating metrology using optical scatterometry.* Journal of Vacuum Science & Technology B, 1997. **15**(2): p. 361-368.
3. Minhas, B.K., et al., *Ellipsometric scatterometry for the metrology of sub-0.1-μm-linewidth structures.* Applied optics, 1998. **37**(22): p. 5112-5115.
4. Delplancke, F., *Automated high-speed Mueller matrix scatterometer.* Applied optics, 1997. **36**(22): p. 5388-5395.
5. Jellison Jr, G., *Spectroscopic ellipsometry data analysis: measured versus calculated quantities.* Thin solid films, 1998. **313**: p. 33-39.
6. Pezzaniti, J. and R. Chipman, *Phase-only modulation of a twisted nematic liquid-crystal TV by use of the eigenpolarization states.* Optics letters, 1993. **18**(18): p. 1567-1569.
7. Pezzaniti, J.L., et al., *Depolarization in liquid-crystal televisions.* Optics letters, 1993. **18**(23): p. 2071-2073.
8. Krishnan, S. and P.C. Nordine, *Mueller-matrix ellipsometry using the division-of-amplitude photopolarimeter: a study of depolarization effects.* Applied optics, 1994. **33**(19): p. 4184-4192.
9. Garcia-Caurel, E., A. De Martino, and B. Drevillon, *Spectroscopic Mueller polarimeter based on liquid crystal devices.* Thin Solid Films, 2004. **455**: p. 120-123.
10. Laude-Boulesteix, B., et al., *Mueller polarimetric imaging system with liquid crystals.* Applied optics, 2004. **43**(14): p. 2824-2832.
11. Bass, M., G. Li, and E. Van Stryland, *Handbook of Optics.* 2010.
12. Moharam, M. and T. Gaylord, *Rigorous coupled-wave analysis of planar-grating diffraction.* JOSA, 1981. **71**(7): p. 811-818.
13. Yee, K.S., *Numerical solution of initial boundary value problems involving Maxwell's equations in isotropic media.* IEEE Trans. Antennas Propag, 1966. **14**(3): p. 302-307.
14. Ahn, S.-W., et al., *Fabrication of a 50 nm half-pitch wire grid polarizer using nanoimprint lithography.* Nanotechnology, 2005. **16**(9): p. 1874.
15. Otani, Y., T. Kuwagaito, and Y. Mizutani. *Surface profile detection with nanostructures using a Mueller matrix polarimeter*. in *Optical Engineering+ Applications*. 2008. International Society for Optics and Photonics.
16. Sanz, J., et al., *Polar decomposition of the Mueller matrix: a polarimetric rule of thumb for square-profile surface structure recognition.* Applied optics, 2011. **50**(21): p. 3781-3788.
17. Muthinti, G.R., B. Peterson, and A.C. Diebold. *Investigation of E-beam patterned nanostructures using Mueller Matrix based Scatterometry*. in *SPIE Advanced Lithography*. 2012. International Society for Optics and Photonics.